Radical Cation of *N*,*N*-Dimethylpiperazine: Dramatic Structural Effects of Orbital Interactions through Bonds

A. M. Brouwer,*,† J. M. Zwier,† C. Svendsen,‡ O. S. Mortensen,‡ F. W. Langkilde,§,⊥ and R. Wilbrandt*,§

Contribution from the Laboratory of Organic Chemistry, Amsterdam Institute of Molecular Studies, Nieuwe Achtergracht 129, 1018 WS Amsterdam, The Netherlands, Physics Department, Odense University, DK-5230 Odense, Denmark, and Plant Biology and Biogeochemistry Department, Risø National Laboratory, PBK-313, Postbox 49, DK-4000 Roskilde, Denmark

Received October 14, 1997

Abstract: The radical cation of *N*,*N*-dimethylpiperazine (DMP) has been studied using time-resolved optical absorption and resonance Raman spectroscopy. Different quantum-chemical methods were used to calculate the molecular structures and vibrational force fields in the ground state of the radical cation and in the resonant excited state. An excellent agreement between theoretical and experimental vibrational frequencies as well as resonance Raman intensities could be achieved. It is concluded that through-σ-bond interaction between the formal lone pair on one amino nitrogen and the odd electron on the other is strong enough to lead to a symmetric charge-delocalized molecular structure of the DMP radical cation, with a chair-type geometry.

1. Introduction

Much of the fundamental insight into the topological aspects of orbital interactions through bonds (TBI) vs orbital interactions through space (TSI) was provided in a series of papers by Hoffmann and co-workers around 1970.[1−3] Hoffmann et al. discussed the stereochemical requirements for efficient TBI but, reverting the argument, also predicted qualitatively what the *structural consequences* of TBI in strongly coupled systems should be.[3]

A classical illustration of the stereochemical requirements for TBI is provided by the well-known rigid cage diamine 1,4-diazabicyclo[2.2.2]octane (DABCO), in which the lone pairs are well aligned with the central C−C bonds, which leads to an easily observable splitting of the lowest energy bands in the photoelectron spectra.[4] It is important to note that in the case of DABCO the neutral molecule already meets the stereochemical requirements for TBI, although the interaction between the doubly occupied lone pair orbitals is not energetically favorable. In the radical cation on the other hand mixing of the two orbitals now containing only three electrons provides considerable stabilization. This is reflected in the relatively low ionization potential[5] and low oxidation potential of DABCO in solution.[6]

Remarkably few other examples were found of TBI in diamines in the extensive studies of Nelsen and co-workers in the early 1970s.[5−7] This is partly due to the fact that photoelectron spectra involve a transition starting from the geometry of the neutral molecule, which may not be favorable for TBI. In that case large splittings are not observed, and information on the ion state must be extracted from the vibrational structure of the spectrum. However, when geometry changes are large, broad, unresolved bands are usually observed. Direct observation of relaxed radical cations was attempted in complementary ESR studies, but these were hampered by the limited chemical stability of the species. Moreover, the interpretation of ESR spectra is not always straightforward, and can be further complicated by molecular dynamics on the ESR time scale, even in low-temperature matrixes.[8]

One way to overcome stability problems is to turn to fast generation and detection methods. Radical cations can be produced using pulse radiolysis or laser flash photolysis techniques, and be detected using time-resolved optical spectroscopy, in particular UV−vis absorption and resonance Raman. With these detection techniques the time-averaging of properties occurs on a much shorter time scale than with ESR, which means that if different molecular conformations are present, a superposition of spectra of the individual species rather than an average spectrum will be obtained.

The usefulness of any experimental approach depends on the possibility of relating the observations with molecular geometric and electronic structure. Here, the spectacular recent development of computational quantum chemistry comes to our aid. In particular, a family of new density functional methods (DFT) has emerged[9,10] which have demonstrated remarkably good performance for molecular structure, molecular vibrations,[11] and thermochemistry.[12] The premise underlying the analysis described in this paper is that if a quantum chemical calculation

† Amsterdam Institute of Molecular Studies.
‡ Odense University.
§ Risø National Laboratory.
⊥ Present address: Astra Hässle AB, S-431 83 Mölndal, Sweden.

(1) Hoffmann, R.; Imamura, A.; Hehre, W. J. *J. Am. Chem. Soc.* **1968**, *90*, 1499.
(2) Hoffmann, R. *Acc. Chem. Res.* **1971**, *4*, 1.
(3) Gleiter, R.; Stohrer, W.-D.; Hoffmann, R. *Helv. Chim. Acta* **1972**, *55*, 893.
(4) Heilbronner, E.; Muszkat, K. A. *J. Am. Chem. Soc.* **1970**, *92*, 3818.
(5) Nelsen, S. F.; Buschek, J. M. *J. Am. Chem. Soc.* **1974**, *96*, 7930.
(6) Nelsen, S. F.; Hintz, P. J. *J. Am. Chem. Soc.* **1972**, *94*, 7114.
(7) Nelsen, S. F.; Buschek, J. M. *J. Am. Chem. Soc.* **1974**, *96*, 6424.
(8) Eastland, G. W.; Ramakrishna Rao, D. N.; Symons, M. C. R. *J. Chem. Soc., Perkin Trans. 2* **1984**, 1551.
(9) Johnson, B. G.; Gill, P. M. W.; Pople, J. A. *J. Chem. Phys.* **1993**, *98*, 5612.
(10) St. Amant, A.; Cornell, W. D.; Kollmann, P. A.; Halgren, T. A. *J. Comput. Chem.* **1995**, *16*, 1483.
(11) Rauhut, G.; Pulay, P. *J. Phys. Chem.* **1995**, *99*, 3093.
(12) Becke, A. D. *J. Chem. Phys.* **1993**, *98*, 5648.

S0002-7863(97)03572-5 CCC: $15.00
Published on Web 04/04/1998

is able to account quantitatively for the electronic absorption spectrum as well as for the vibrational spectrum of a radical cation, then it is likely that the computed molecular geometry and electronic structure are also correct.

N,*N*-Dimethylpiperazine (DMP) is chosen as the subject of this paper because it is a nice example of a molecule that shows only small splittings in the lone pair ionization energies due to an unfavorable geometry for TBI, while its radical cation (DMP^+) undergoes a large structural reorganization, allowing efficient TBI to occur.[13] This leads to a delocalization of charge and spin density over the equivalent amino groups, in contrast to some piperazine radical cations with aromatic substituents.[14,15] In this paper we shall put our preliminary conclusions concerning this species on a much firmer basis, using two isotopically substituted derivatives to ascertain the assignments of the vibrational spectra. On the computational side, density functional calculations are used in the present work because of the crucial role of electron correlation in the species studied.[16] Having established the molecular geometric structure of DMP^+, we shall discuss its electronic structure. Finally, a brief comparison with the Raman spectra of the neutral molecule will be made.

2. Experimental and Computational Methods

2.1. Materials. *N*,*N*-Dimethylpiperazine was used as received from Aldrich. The deuterated derivatives were synthesized by reduction with $LiAlD_4$ in THF[17] of 1,4-dimethylpiperazine-2,5-dione to give the 2,2,5,5-d_4 isotopomer and of diethyl 1,4-piperazinedicarboxylate to yield the methyl-d_6 species. All reagents were purchased from Aldrich. The isotopomers were purified using preparative gas chromatography. ^1H NMR showed the complete absence of the signals of the hydrogen atoms that were replaced by deuterium. Thus, we estimate the deuterium content to be at least 95%. Moreover, in the vibrational spectra of the radical cations no bands are seen that cannot be accounted for.

2.2. Generation and Detection of Radical Cations. All measurements were carried out in aerated CH_3CN solutions (Merck, spectroscopic grade) at ambient temperature. DMP (5×10^{-3} M) was oxidized to its radical cation by the radical cation of biphenyl. For the Raman experiments this transient oxidant was generated by direct photoionization of biphenyl (4.3×10^{-4} to 1×10^{-3} M) at 266 nm (Quantel 481A Nd:YAG laser) or 248 nm (Lambda Physik LPX 220i Excimer laser, KrF, 9 mJ, 20 ns pulses). For transient absorption experiments, in which a much larger volume of solution is probed, the use of a cosensitization technique[18] is more convenient. These experiments will be described in more detail elsewhere. DMP^+ is formed in a pseudo-first-order process within <100 ns. It is important to note that a reducing equivalent is generated together with the radical cations, probably O_2^-, which is able to react in a relatively slow bimolecular process with the radical cations via electron transfer, regenerating the starting neutral molecules within a few microseconds. The well-known unimolecular decomposition reactions typical of saturated amines,[6,19] which in most cases lead to irreversible cyclic voltammograms, apparently cannot compete on this time scale. As a result the measurement solutions are chemically remarkably stable and can take thousands of laser pulses without noticeable decomposition.

Resonance Raman spectra of transient radical cations in the region 350−1750 cm^{-1} were excited 70−160 ns after the photolyzing light pulse, at a wavelength of 620 (DMP-d_0), 600 (DMP-d_6), and 595 (DMP-d_4) nm, with pulses of 1.0−2.0 mJ/pulse energy (15 ns pulses, 5 Hz repetition rate) from an excimer (Lambda Physik EMG102E) pumped dye laser (Lambda Physik FL3002). Scattered Raman light was collected at right angles to the laser beam, passed through a band-pass filter (Schott RG645 or RG630) and a polarization scrambler, and dispersed in a home-built 0.6 m spectrograph. The spectral resolution was 10 cm^{-1}. Spectra were detected by a gated intensified optical multichannel analyzer (Spectroscopy Instruments OSMA IRY-700) with 700 active channels. The wavenumber scale was calibrated using the Raman spectrum of indene as a reference. Data handling was performed on a PDP11/23 computer. A sample was exposed to 1000 laser pulses, and spectra from four samples were averaged. The final spectra were obtained after subtraction of solvent bands. The spectra were not corrected for the absorption of the RG-filters, the absorption of the sample, and the wavelength dependence of the sensitivity of our detection system.

2.3. Raman Spectra of DMP. The FT-Raman spectrum of neat DMP was measured at a resolution of 4 cm^{-1} on a Bruker RFS100 FT-Raman spectrometer, using a Nd:YAG laser (400 mW, 1064 nm). The preresonance Raman spectrum of neutral DMP was recorded using a solution of 0.37 M DMP in acetonitrile. The fourth harmonic of the Nd:YAG laser at 266 nm was used for excitation. The spectral resolution in this case was 20 cm^{-1}.

2.4. Computational Tools. Ab initio calculations were carried out using the Gaussian programs,[20,21] with Hartree−Fock (HF) theory followed by MP2 correction for correlation energy, and using the BLYP and B3LYP density functionals.[12,22,23] The standard 6-31G(d) basis set was used throughout. For visualization of orbitals we used Spartan 4.1 (Wavefunction, Inc., Irvine, CA).

3. Experimental Results

The optical absorption spectrum of DMP^+ in acetonitrile solution, shown in Figure 1A, consists of a broad band centered at 600 nm, and is very similar to the spectrum reported of the same species produced by pulse radiolysis in an alkane glass,[24] for which the absorption coefficient was reported to be 1800 M^{-1} cm^{-1}.[24] Resonance Raman spectra of DMP^+ and two isotopomers obtained in resonance with this band are shown in Figure 1B−D.

A comparison of the preresonance Raman spectrum of the neutral DMP molecule (266 nm) with the off-resonance FT-Raman spectrum (1064 nm) is presented in Figure 2.

The interpretation of the Raman spectra will be discussed in section 6.

4. Computed Molecular Geometries of DMP^+ and DMP

When considering the possible structures of the radical cation of DMP several aspects come to mind (see Figure 3). If the charge is localized on one amino group, this can be expected to be essentially planar, and the other neutral amino group will be pyramidal. A chair conformation seems most probable in this case. If on the other hand the charge is delocalized, this is likely to induce geometry changes characteristic of either

(13) Brouwer, A. M.; Langkilde, F. W.; Bajdor, K.; Wilbrandt, R. *Chem. Phys. Lett.* **1994**, *225*, 386.
(14) Nelsen, S. F.; Yunta, M. J. R. *J. Phys. Org. Chem.* **1994**, *7*, 55.
(15) Brouwer, A. M.; Wiering, P. G.; Zwier, J. M.; Langkilde, F. W.; Wilbrandt, R. *Acta Chem. Scand.* **1997**, *51*, 217.
(16) Brouwer, A. M.; Krijnen, B. *J. Org. Chem.* **1995**, *60*, 32.
(17) Ram, S.; Ehrenkaufer, R. E. *Tetrahedron Lett.* **1985**, *26*, 5367.
(18) Schaap, A. P.; Siddiqui, S.; Prasad, G.; Palomino, E.; Lopez, L. *J. Photochem.* **1984**, *25*, 167.
(19) Lindsay Smith, J. R.; Masheder, D. *J. Chem. Soc., Perkin Trans. 2* **1977**, 1732.
(20) Gaussian 92/DFT: Frisch, M. J.; Trucks, G. W.; Schlegel, H. B.; Gill, P. M. W.; Johnson, B. G.; Wong, M. W.; Foresman, J. B.; Robb, M. A.; Head-Gordon, M.; Replogle, E. S.; Gomperts, R.; Andres, J. L.; Raghavachari, K.; Binkley, J. S.; Gonzalez, C.; Martin, R. L.; Fox, D. J.; Defrees, D. J.; Baker, J.; Stewart, J. J. P.; Pople, J. A., Pittsburgh, PA, 1993.
(21) Gaussian 94: Frisch, M. J.; Trucks, G. W.; Schlegel, H. B.; Gill, P. M. W.; Johnson, B. G.; Robb, M. A.; Cheeseman, J. R.; Keith, T.; Petersson, G. A.; Montgomery, J. A.; Raghavachari, K.; Al-Laham, M. A.; Zakrzewski, V. G.; Ortiz, J. V.; Foresman, J. B.; Cioslowski, J.; Stefanov, B. B.; Nanayakkara, A.; Challacombe, M.; Peng, C. Y.; Ayala, P. Y.; Chen, W.; Wong, M. W.; Andres, J. L.; Replogle, E. S.; Gomperts, R.; Martin, R. L.; Fox, D. J.; Binkley, J. S.; Defrees, D. J.; Baker, J.; Stewart, J. J. P.; Head-Gordon, M.; Gonzalez, C.; Pople, J. A., Pittsburgh, PA, 1995.
(22) Becke, A. D. *Phys. Rev. A* **1988**, *38*, 3098.
(23) Lee, C.; Yang, W.; Parr, R. G. *Phys. Rev. B* **1988**, *37*, 785.
(24) Gebicki, J.; Marcinek, A.; Stradowski, C. *J. Phys. Org. Chem.* **1990**, *3*, 606.

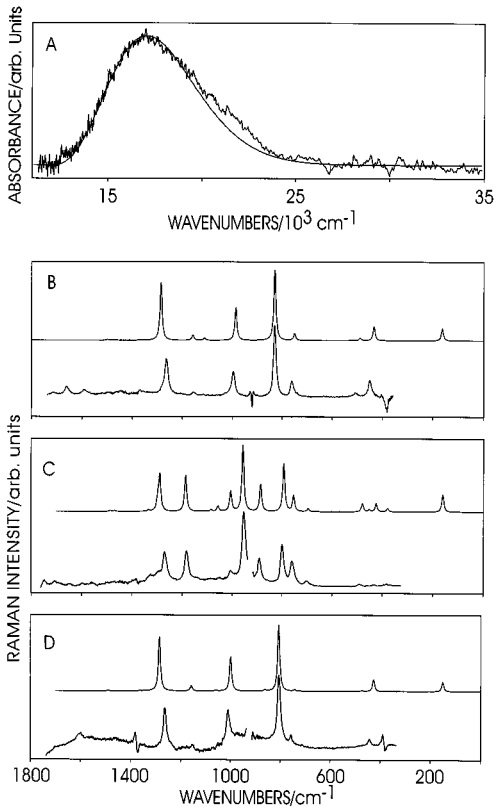

Figure 1. (A) Experimental and computed optical absorption spectrum of DMP^+ and (B−D) time-resolved resonance Raman spectra of the radical cations of (B) DMP-d_0, (C), DMP-d_4, and (D) DMP-d_6, produced via photoionization of biphenyl at 248 nm, probe wavelength 620 (DMP-d_0), 600 (DMP-d_6), and 595 (DMP-d_4) nm, pump−probe delay 70−160 ns. The corresponding computed spectrum (B3LYP/6-31G*) is shown above each experimental Raman spectrum. See section 6.2 for a discussion of intensities.

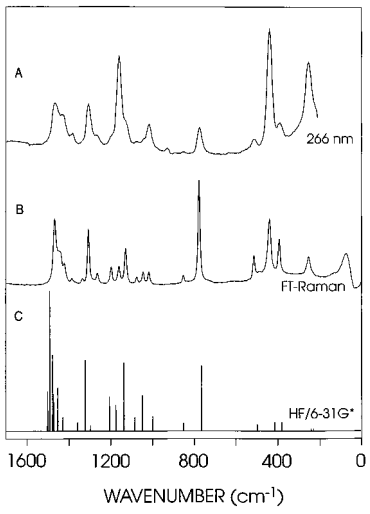

Figure 2. (A) Preresonance Raman spectrum (266 nm) of DMP in acetonitrile (0.37 M), (B) FT-Raman spectrum of neat DMP, and (C) computed spectrum (HF/6-31G*, frequencies scaled × 0.90).

dominant through-bond or through-space coupling. The latter requires a boat type conformation to bring the nitrogen atoms close together. This type of structure has been proposed for the radical cations of 1,4-dithiane[25] and 1,4-dioxane.[26] For 1,4-

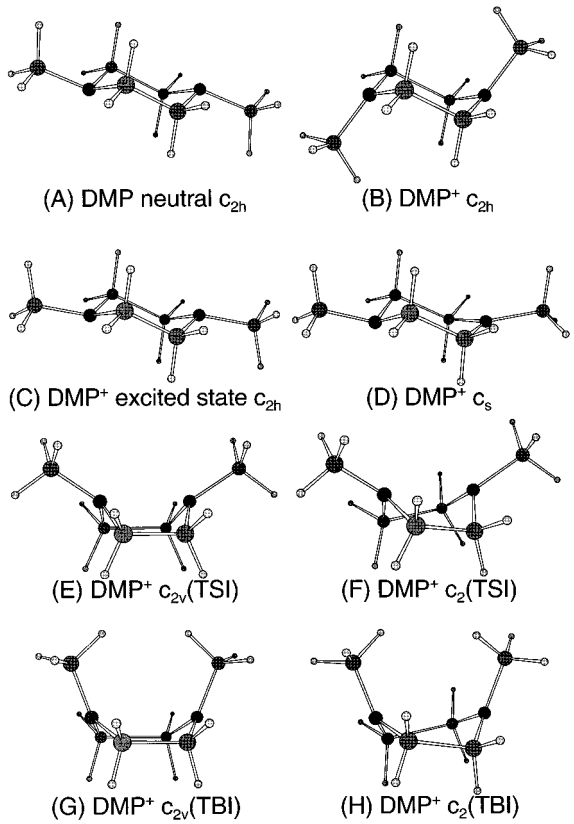

Figure 3. Characteristic structures of DMP (A) and its radical cation (B−H), computed at the HF/6-31G* level: (A) neutral molecule, C_{2h} symmetric chair, (B) radical cation C_{2h} symmetric chair, (C) ^2B_u radical cation excited state, (D) C_s symmetry-broken chair, (E) boat, optimal for through-space interaction (C_{2v}(TSI)), (F) twisted-boat, optimal for through-space interaction (C_2(TSI)), (G) boat, optimal for through-bond interaction (C_{2v}(TBI)), (H) twisted-boat, optimal for through-bond interaction (C_2(TBI)).

through-bond interaction the optimal transoid orientation of the connecting C−C bond[2] cannot be achieved in the six-membered ring system. The linkage is either gauche (in chair forms) or syn (in boats). We have previously reported[13] that the charge-delocalized chair form (C_{2h}) is the form of lowest energy for the DMP radical cation, provided that electron correlation (MP2) is taken into account. In this paper we will give a more complete characterization of the structural features of the characteristic conformations. Furthermore, density functional theory is used to asses the importance of electron correlation.

Table 1 gives an overview of the various stationary points located on the energy surfaces of DMP^+ at different levels of theory. Some representative examples are shown in Figure 3. All structures were characterized by a frequency calculation, except those obtained with MP2 theory. Important aspects of the structure are the length of the "central" C−C bond, which can be indicative of the occurrence of through-bond interaction,[3,13,16,27] the sum(s) of the bond angles at the N atoms ($\sum$N), which are related to the hybridization (typically, sp^3 for saturated amines ($\sum N \approx 328.4°$), sp^2 for radical cations ($\sum N \approx 360°$)), and the distance between the N atoms, which may point to the occurrence of a 3-electron bond in boat-type conformations.

The chair form of DMP^+ (C_{2h} symmetry, Figure 3B) shows intermediate pyramidalization of the amino groups, with the methyl groups oriented toward the axial face. When the geometry is optimized starting from that of the neutral molecule

(25) Shida, T.; Momose, T. *J. Mol. Struct.* **1985**, *126*, 159.
(26) Bonazzola, L.; Michaut, J. P.; Roncin, J. *New J. Chem.* **1994**, *18*, 1163.
(27) Krijnen, B.; Beverloo, H. B.; Verhoeven, J. W.; Reiss, C. A.; Goubitz, K.; Heijdenrijk, D. *J. Am. Chem. Soc.* **1989**, *111*, 4433.

Table 1. Optimized Structures of DMP and DMP^+ at Different Levels of Theory[a]

	HF-3/21G	HF/6-31G*	MP2/6-31G*	BLYP/6-31G*	B3LYP/6-31G*
			Neutral, C_{2h}		
energy	−342.31990	−344.23086	*b*	−346.35301	−346.55200
freq	109	120		115	118
r(CC)	1.528	1.521		1.539	1.527
∑N	337.9	335.4		334.0	334.3
			DMP^+ C_{2h}		
energy	−342.08878	−343.98296	−345.10009	−346.11973	−346.30310
freq	119	127	*b*	99	109
r(CC)	1.643	1.618	1.598	1.617	1.608
∑N	354.2	352.2	349.4	351.5	351.5
			DMP^+ excited-state C_{2h}		
energy	*b*	−343.94331	−345.06456	−346.09661	−346.27585
freq		73	*b*	63	335i, 73
r(CC)		1.511	1.515	1.536	1.523
∑N		346.7	344.5	346.5	346.6
			DMP^+ C_s		
energy	−342.10075	−344.00167	−345.07185	−346.11841	−346.30154
relative *E*	−7.51	−11.74	17.72	0.83	0.97
freq	38i[c]	13	*b*	115i[c]	*b*
r(CC)	1.542	1.527	1.545	1.617	1.607
∑N1	359.8	359.8	357.9	355.6	355.1
∑N2	341.8	336.4	334.7	350.9	350.8
			DMP^+ C_{2v}(TBI)		
energy	−342.06669	−343.96020	−345.07606	−346.10128	−346.28337
relative *E*	13.86	14.28	15.07	11.58	12.38
freq	143i, 101i,[c] 54	119i,[c] 82i, 15	*b*	81i, 51i,[c] 72	85i,68i,[c] 58
r(NN)	2.633	2.688	2.691	2.743	2.710
r(CC)	1.705	1.667	1.645	1.666	1.654
∑N	356.4	355.3	354.4	354.8	355.0
			DMP^+ C_2 (TBI)		
energy	−342.06829	−343.96156	*b*	−346.10271	−346.28485
relative *E*	12.85	13.43		10.68	11.45
freq	53i,[c] 70	38		49	60
r(NN)	2.655	2.683		2.774	2.731
r(CC)	1.695	1.653		1.633	1.627
∑N	355.8	353.6		353.1	353.0
			DMP^+ C_{2v}(TSI)		
energy	−342.06947	−343.96505	−345.06871	−346.10014	−346.28150
relative *E*	12.12	11.23	19.69	12.29	13.55
freq	44i, 104	74i, 100	*b*	109i, 74	111i, 74
r(NN)	2.108	2.216	2.384	2.583	2.499
r(CC)	1.542	1.529	1.528	1.546	1.534
∑N	351.5	349.7	346.9	349.1	348.9
			DMP^+ C_2(TSI)		
energy	−342.06954	−343.96539	−345.07207	−346.10286	−346.28371
relative *E*	12.07	11.02	17.58	10.59	12.17
freq	62	91	*b*	53	50
r(NN)	2.114	2.230	2.553	2.739	2.642
r(CC)	1.540	1.526	1.522	1.542	1.529
∑N	351.8	350.3	349.8	352.9	352.0

[a] For each structure the following are given: energy (hartree), energy relative to the C_{2h} form (kcal/mol); any imaginary, and lowest real vibrational frequencies (cm^{-1}); N−N distance (*r*(NN)); bond length *r*(C2−C3) (=*r*(C5−C6)) (*r*(CC)) (Å); sum(s) of bond angles ∑N at the nitrogen atoms (deg). [b] Not determined. [c] The imaginary frequency corresponds to a methyl rotation.

(Figure 3A), in which the methyl groups are equatorial, a spontaneous nitrogen inversion occurs. For the boat conformations (C_{2v} symmetry) and the twisted-boats (C_2) two kinds of methyl orientation give rise to distinct energy minima, as shown in Figure 3. The asymmetric chair conformation (C_s) is the lowest energy structure at the HF level (Figure 3D), and appears to correspond to a local minimum on the MP2/6-31G* surface. With DFT calculations, however, optimization led smoothly to a charge-delocalized structure which differs from the C_{2h} form only in the rotational orientation of one of the methyl groups. The energy is only slightly higher than that of the C_{2h} structure.

In view of the possibility of a 3-electron−2-center bond (through-space interaction) we performed optimizations of boat structures starting from geometries with the methyl groups equatorial. At the HF/3-21G level we could indeed locate a boat conformation with a short distance (2.1 Å) between the nitrogen atoms (C_{2v}(TSI)). In this case the energy difference with the twisted boat is negligible. Taking these through-space bonded structures as starting points for HF optimizations with the 6-31G* basis set gave structures with somewhat larger N−N distance (2.2 Å) (Figure 3E,F), but using correlated models a substantial increase was found of the N−N distance up to 2.7 Å, almost as large as in the "TBI" structures discussed below. In all of these structures the amino groups have an intermediate hybridization, and the methyl groups are oriented more or less equatorially. The boat forms are transition states between two enantiomeric twisted-boat forms (C_2 symmetry), which are true minima, but the energy differences are small. In any case, the

computed relative energies of all boat forms, regardless of the level of theory used, make it a priori unlikely that the DMP radical cation attains this kind of conformation.

A second group of boat structures are those in which the methyl groups are in a pseudoaxial orientation (Figure 3G,H). These species, denoted as $C_{2(v)}$(TBI) are characterized by a relatively long C2−C3 bond, the signature of dominant TBI. In these boat conformations the through-bond coupling may be more effective than in the chair form, because the coupling path involves a syn rather than a gauche linkage. This leads to considerably longer C−C bonds in these boat forms. The opposing TSI, however, leads to a smaller orbital splitting than in the chair (see below).

The calculations discussed here all pertain to isolated molecules, while experiments were all performed using solutions in acetonitrile. This polar solvent may exert different stabilizing effects on different molecular structures; in particular it may be expected to favor structures with a more localized charge. To estimate the importance of this effect, we carried out calculations using the self-consistent isodensity polarized continuum method (SCIPCM).[28] UHF/6-31G* wave functions and the gas-phase optimized geometries were used. Indeed, with a dielectric constant of 37 (acetonitrile) the C_s structure (Figure 3D) is computed to have the largest solvation energy, 53.2 kcal/mol, while the other three structures have almost the same solvation energies, viz., 50.6 kcal/mol for C_{2h}, 49.7 for C_2(TSI), and 50.2 for C_2(TBI). The solvation energy difference in favor of the charge-localized structure of ca. 2.6 kcal/mol is small relative to the energy differences between the C_{2h} and C_s forms at correlated levels, so in the present case solvent-induced charge localization is not likely to occur. In another calculation we attempted to evaluate how strong the solvent-induced charge-localization affects the electron density distribution. For this purpose UB3LYP/6-31G* was used at the HF-optimized C_s geometry, which in contrast to the B3LYP optimized geometry favors localization of charge and spin on the planar amino group. In the gas phase, the spin densities on the nitrogen atoms are 0.11 and 0.72, respectively. Applying a dielectric continuum (SCIPCM) leads to an increased polarization of the density distribution, as indicated by the nitrogen spin densities of 0.05 and 0.79, respectively. In the B3LYP gas phase optimized geometry, dissymmetric only due to the orientation of the methyl groups, spin densities on both nitrogens are similar (0.41 and 0.36). It would have been interesting to see if the presence of the solvent (simulated as a dielectric continuum) could lead to a local minimum with B3LYP for the C_s structure (similar to the HF one), but unfortunately, attempts to optimize the geometry with the continuum model were not successful.

5. Electronic Structure and Optical Absorption Spectrum of the DMP Radical Cation

5.1. Electronic Structure. The electronic structure of DMP and its radical cation can be discussed on the basis of the two highest occupied MOs, which are in essence nitrogen lone pair orbitals. In the neutral *N*,*N*-dimethylpiperazine molecule the splitting of the lone pair ionization energies in the photoelectron spectrum is hardly observable.[5] The splitting of the computed orbital energies at the HF/6-31G* level is $\Delta\epsilon = 0.15$ eV, in agreement with this experimental result. As shown in Figure 4, the HOMO can be characterized as the symmetric combination of the lone pairs which mixes with the σ-bond, and the second highest occupied MO (HOMO − 1) is the antisymmetric combination, as expected for through-bond interaction involving an odd number of σ-bonds.[2]

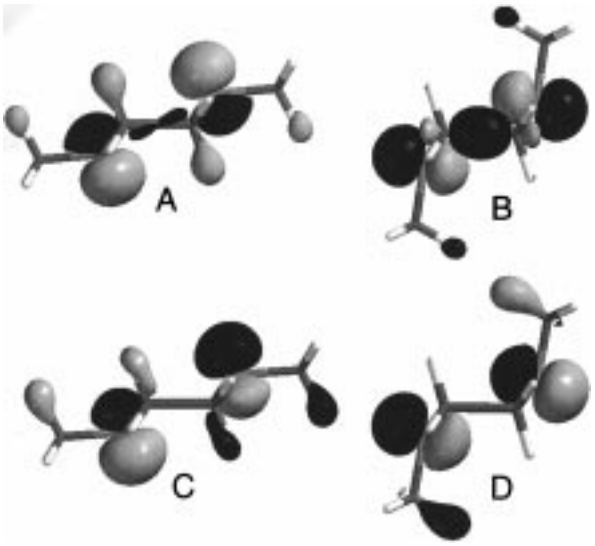

Figure 4. Graphical representation of molecular orbitals (0.065 e Å^{-3}) of DMP and its radical cation: (A) HOMO neutral, (B) HOMO (SOMO) DMP$^+$, (C) HOMO − 1 neutral, (D) HOMO − 1 DMP$^+$. The orbitals were evaluated using RHF/6-31G* calculations (i.e., for the neutral molecule) at the HF optimized geometries of the different species.

In contrast to the situation in the neutral molecule, in the DMP radical cation a considerable amount of energy can be gained when the frontier MOs are allowed to mix strongly, because the HOMO − 1 is doubly occupied while the HOMO (SOMO) contains only one electron. This forms the driving force for the considerable structural reorganization that is predicted by all ab initio calculations. The concomitant change in the appearance of the MOs is illustrated in Figure 4.

It should be noted that the symmetric structures at the HF level are somewhat artificial in the sense that the wave function was constrained to be symmetric. When this constraint is lifted, breaking of the spatial symmetry results in a lowering of the energy by 2.3 kcal/mol for the C_{2h} structure and 4.6 kcal/mol for the C_2(TSI) form. In principle, use of the unstable symmetric wave function in MP2 calculations or in calculation of the force constants should not give valid results. Nevertheless, the force constants for the totally symmetric vibrations of the C_{2h} chair were found to be very useful. For nontotally symmetric vibrations, however, very peculiar results are found, which are evidently a result of the inherent instability of the wave function. It may be interesting to note that application of a different constraint, viz., the use of restricted Hartree−Fock, has practically no effect on the results. The UHF wave functions show virtually no spin contamination: $\langle S^2\rangle = 0.76$. In contrast to the pure HF wave function, the mixed HF−DFT UB3LYP calculation did not show instabilities.

5.2. Nature of the Electronic Transition. The optical absorption band at 600 nm (2.07 eV, 47.6 kcal/mol) can be assigned to a 1-electron transition from the doubly occupied HOMO − 1 (b_u) to the SOMO (a_g). Other transitions cannot explain such a low-energy absorption band because they involve either excitation from low-lying σ-orbitals or excitation into Rydberg or σ^* levels. The orbital energy splitting (2.82 eV) may serve as a first approximation to the vertical $A_g \rightarrow B_u$ excitation energy. Due to the different symmetries of the orbitals, the B_u excited state can be calculated directly with single-determinant methods. The vertical excitation energies

(28) Foresman, J. B.; Keith, T. A.; Wiberg, K. B.; Snoonia, J.; Frisch, M. J. *J. Phys. Chem.* **1996**, *100*, 16098.

Table 2. Computed Energies (kcal/mol) (relative to Those of the Optimized A_g Ground State) of the B_u Excited State of DMP^+ (C_{2h}) and of the A_g Ground State at the B_u Optimized Geometry[a]

			energy		
state	geometry	HF	MP2//HF	BLYP	B3LYP
B_u	A_g optimized	60.60	51.62	39.32	44.59
B_u	B_u optimized	24.88	22.30	14.50	17.10
A_g	B_u optimized	20.26	17.71	10.33	12.54

[a] The 6-31G* basis set was used for all calculations.

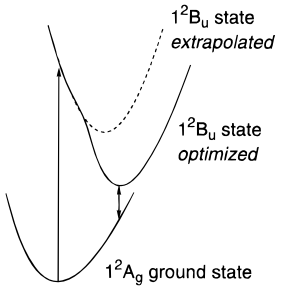

Figure 5. Energy curves of DMP^+ (C_{2h}) in ground and excited states, schematically illustrating the large reorganization energies, the small energy gap at the relaxed excited-state geometry, and the difference between optimized and extrapolated excited-state geometries (see section 6.2).

calculated in this way are given in the first data column of Table 2. Geometry optimization of the excited state leads to a large energy lowering, and a strongly reduced gap with the A_g state. The energies of the optimized B_u state and of the ground state at the B_u optimized geometry are also listed in Table 2. Note that although all optimized structures have C_{2h} symmetry, a rotation of the methyl groups is needed to arrive at the fully optimized B_u species.

The nature of the geometry change after excitation is readily understood considering the 2-orbital−3-electron picture: when 2 electrons reside in the higher level, and only one is in the lower-energy MO, the natural response is to reduce the splitting of the levels. In fact, the optimized B_u species looks much like the neutral molecule. The structure is shown in Figure 3C, and geometric data are included in Table 1. For example, with the B3LYP method, the CC bond length is found to be 1.523 Å and the pyramidalization puts the methyl groups toward the equatorial side, the sum of the bond angles at nitrogen being 346.6°. At this geometry the energy gap between the states is small, as shown in the last entries of Table 2, and illustrated schematically in Figure 5. As a result, the lifetime of the upper state is likely to be exceedingly short.

The excitation energies computed for the C_{2h} structure (Table 2) are in good agreement with the experimental data. The HF value is somewhat too high, but when electron correlation is taken into account, the agreement is improved. For comparison, we computed the excitation energies for the (twisted) boat forms at the HF/6-31G* level. The predicted excitation energies are 47.5 kcal/mol for the through-space bonded form C_2(TSI) and 43.4 kcal/mol for the C_2(TBI) conformer. Clearly, these values are much lower than that for the C_{2h} form, and considering the further lowering effect of electron correlation, they are too low with respect to the experimental excitation energy. This can be taken as a further argument against the occurrence of boat conformations.

If DMP^+ would adopt the asymmetric charge-localized C_s structure, one would expect the transition to be of a charge-transfer nature. The excitation energy should in that case be equal to the reorganization energy, which is composed of an internal and a solvent contribution. Such a charge-transfer transition was indeed found in 1,4-bis(4-(dimethylamino)-phenyl)piperazine[14] at ca. 1.3 eV. The internal reorganization energy for a saturated amine is larger than that for an aromatic amine. We have estimated the difference to be ca. 0.7−0.8 eV,[29] so a charge-localized structure is not a priori in conflict with the wavelength position of the observed absorption band. The absorption coefficient of 1800 M^{-1} cm^{-1} is much greater than that of the CT-band in 1,4-bis(4-(dimethylamino)phenyl)-piperazine (ca. 100 M^{-1} cm^{-1}),[14] but this can be explained by the greater confinement of the frontier orbitals to the nitrogen atoms, which leads to a much greater electronic coupling. Absorption coefficients of the same order of magnitude have also been found in closed-shell electron-donor−acceptor molecules with similar structures.[27] Thus, although the optical absorption spectrum is in perfect agreement with the calculations for the C_{2h} form, by itself it does not allow the rejection of the symmetry-broken C_s form as a possible structure of DMP^+.

6. Raman Spectra

6.1. Assignments of the Resonance Raman Spectrum of DMP^+ and Isotopomers. We have previously reported that the experimental resonance Raman spectrum of DMP^+ could be readily explained using only totally symmetric vibrations of the C_{2h} structure, calculated at the HF/6-31G* level. With the availability of two isotopically substituted derivatives we can further test the validity of this conclusion. The computed vibrational frequencies of DMP^+ (C_{2h}) are compared with the experimental data in Table 3.

The 25 fundamental frequencies available were used to derive optimized linear scaling factors of 0.902 for HF, 1.01 for BLYP, and 0.974 for B3LYP. These scale factors are only slightly larger than those published recently for a large test set of neutral molecules.[30] Root-mean-square (rms) deviations are 19 cm^{-1} for HF, 18 cm^{-1} for BLYP, and 14 cm^{-1} for B3LYP calculations. The largest absolute deviation was 28 cm^{-1} at the HF level, 31 cm^{-1} with the BLYP method, and only 22 cm^{-1} with the B3LYP functional.

In addition to the fundamentals reported in Table 3, combination bands were found at 1591, 1660, and 1710 cm^{-1} for the d_0 species, at 1559, 1596, 1648, and 1706 cm^{-1} for the d_4 species, and at 1604 cm^{-1} for the d_6 isotopomer. In the calculations of the spectra the combination bands were not taken into consideration.

The computed totally symmetric normal modes of vibration for DMP^+ (C_{2h}) are presented in Figure 6. The modes shown are from the B3LYP/6-31G* calculation, but those obtained with HF and BLYP are very similar.

The computed frequencies for the C_{2h} structure agree very well with the experimental data, but we should be prepared to consider the possibility that other structures may fit just as well. For the charge-localized C_s chair, which exists only at the HF level, we have previously shown that the low-frequency region in the d_0 spectrum cannot be explained by the computed spectrum.[13] Boat structures, or rather twisted boats of C_2-symmetry, should still be considered. We note that for the d_4 isotopomer the number of bands in the experimental spectrum is much greater than for the other two, which is consistent with the C_{2h} structure because the lower symmetry of the nuclear masses in the d_4 species allows b_g vibrations to appear in the spectrum. This effective change in symmetry upon deuteriation does not occur for the twisted boats, so a change in the number

(29) Brouwer, A. M. *J. Phys. Chem. A* **1997**, *101*, 3626.
(30) Scott, A. P.; Radom, L. *J. Phys. Chem*. **1996**, *100*, 16502.

Table 3. Experimental and Computed Fundamental Vibrational Frequencies (cm^{-1}) of DMP^+ and the 2,2,5,5-d_4 and Methyl-d_6 Deuteriated Isotopomers[a]

d_0				d_4				d_6			
exptl	B3L	BLYP	HF	exptl	B3L	BLYP	HF	exptl	B3L	BL	HF
					a_g Modes						
b	163	164	172	*b*	160	160	169	*b*	149	152	158
451	434	433	431	435	423	425	420	442	425	424	422
508	490	485	487	491	479	476	475	*c*	473	467	472
761	751	751	733	702	695	697	681	757	741	740	727
830	830	818	817	800	792	785	782	806	806	796	787
995	986	988	991	953	956	959	959	1010	998	996	1004
c	1111	1118	1117	*c*	1115	1122	1125	*c*	861	865	866
1155	1158	1161	1163	1181	1185	1183	1191	1153	1157	1155	1162
1263	1285	1296	1291	1007	1005	1009	1005	1262	1285	1294	1290
c	1362	1371	1369	1332	1333	1333	1354	*c*	1363	1370	1368
1443[d]	1436	1454	1443	*c*	1438	1452	1446	*c*	1103	1110	1108
c	1469	1484	1471	*c*	1469	1481	1446	*c*	1058	1067	1060
c	1498	1514	1507	*c*	1487	1499	1494	*c*	1492	1504	1501
					b_g Modes						
				c	135	160	122				
				c	377	375	378				
				c	451	450	447				
				761	753	754	747				
				892	885	890	885				
				1052	1056	1061	1057				
				c	1083	1086	1089				
				1269	1289	1285	1291				
				c	1296	1301	1313				
				c	1476	1494	1476				

[a] Frequency scaling factors were 0.974 for B3LYP/6-31G*, 1.01 for BLYP, and 0.902 for HF. Only totally symmetric modes are reported (a_g for d_0 and d_6, a_g and b_g for d_4). The frequencies are arranged in increasing order for the parent isotopomer, those of the d_4 and d_6 species according to their similarity with the corresponding normal mode of d_0. [b] Outside of the detectable spectral range. [c] Not observed. [d] Weak band, not included in the fit of the scale factor.

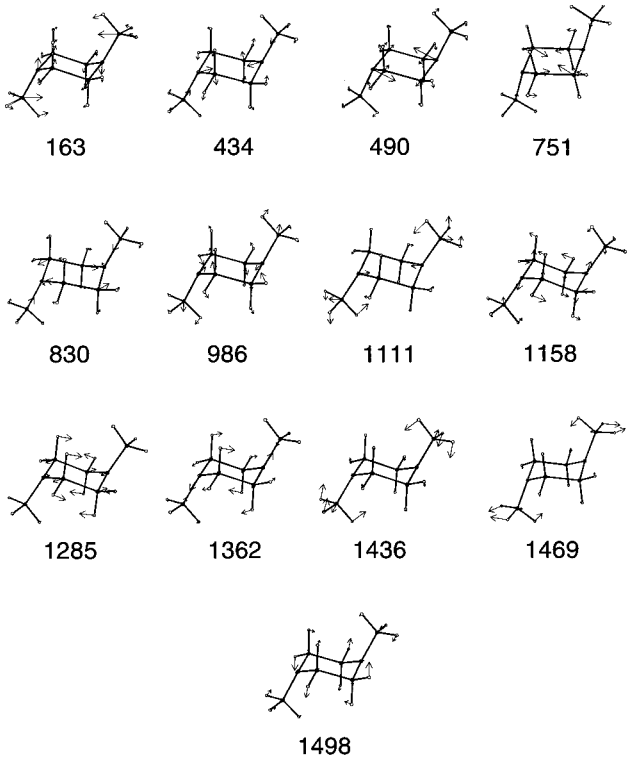

Figure 6. Totally symmetric (a_g) normal modes of vibration of DMP^+ (C_{2h}) calculated at the B3LYP/6-31G* level. Computed frequencies (cm^{-1}) scaled × 0.974.

of active vibrations is not expected for these, contrary to the observation.

Closer inspection of the frequencies calculated for the boat forms (i.e., the C_2 structures) shows that these cannot account for the spectra in a satisfactory way. Comparing experimental and optimally scaled frequencies for all isotopomers, the C_2-(TSI) structure (which only exists with a short N−N distance at the HF level) gives an rms deviation of 23 cm^{-1}. This is not much larger than that found for the C_{2h} structure, but there are several large absolute deviations (up to 51 cm^{-1}) which is not the case for the C_{2h} form. Moreover, the predicted intensities do not agree at all with the observed ones (see below). Looking at the B3LYP results for the C_2 forms, the disagreement is so obvious that we refrained from a statistical analysis. Deviations as large as 50 cm^{-1} are found, while the C_{2h} form gives errors of at most 22 cm^{-1}. The vibrational frequencies strongly support the conclusion indicated by the relative energies that the C_{2h} structure is the correct one.

6.2. Intensities of the Bands in the Resonance Raman Spectra of DMP^+. In the present experimental work we have not attempted to obtain quantitative Raman intensities. The scattered light may in part be reabsorbed by the DMP radical cation present in high concentration, and the collection optics as well as the detection system have a wavelength-dependent response. However, because all these effects can be expected to be a smooth function of wavelength, and in part cancel each other, the qualitative picture of relative intensities should be reasonable.

The theoretical calculation of optical absorption spectra and resonance Raman intensities is usually done using the Born−Oppenheimer and Condon approximations together with the assumption of harmonic nuclear potential surfaces. The present work does not go beyond these approximations. For polyatomic molecules with many vibrational degrees of freedom the often used sum-over-states method[31] is intractable. In this case, the elegant wave packet formulation of optical absorption and resonance Raman scattering developed by Tannor and Heller[32]

(31) Siebrand, W.; Zgierski, M. Z. *J. Chem. Phys.* **1979**, *71*, 3561.

can be used. In their formulation, the vibrational Hamiltonians are written in terms of dimensionless normal coordinates. Each of the potential surfaces of the vibrational Hamiltonians is characterized by a set of normal coordinates and vibrational frequencies. The relative position of the potential surfaces involved in the optical processes is characterized by the Duschinsky rotation matrix and a set of dimensionless displacements. In the following, the parameters which characterize the potential surfaces and their relative positions are referred to as the *vibrational parameters*.

In the present work, the vibrational parameters of the radical cation of DMP have been obtained by use of quantum chemical calculations. Two different approaches for the determination of the vibrational parameters are used, which we here denote as the *vertical approach*[33] and the *adiabatic approach*. In the vertical approach, only the ground-state geometry is optimized and excited-state properties are evaluated at the optimized geometry of the ground-state only. Two degrees of sophistication are here used within the vertical approach, in the following denoted by the *vertical Hessian* and the *vertical gradient approach*. The *vertical Hessian approach* uses the molecular gradient and Hessian of the excited electronic state evaluated at the optimized geometry of the ground electronic state together with the Hessian of the ground electronic state evaluated at the same geometry. In this approach both the ground- and excited-state potential surfaces are expanded to second order in the nuclear coordinates around the same point, which is the optimized geometry of the ground electronic state. The vibrational parameters obtained in this way are then used as input parameters for the evaluation of optical absorption spectra and resonance Raman intensities by means of wave packet propagation techniques. In the *vertical gradient approach*, only the gradient of the excited state at the ground-state optimized geometry is taken into account while the force field in the excited state is assumed to be identical to that of the ground state. Also, in contrast to the vertical Hessian approach, here no proper removal of translational and rotational degrees of freedom is carried out. The vibrational parameters which in this case are the displacements and frequencies are then used to calculate the Raman intensities by employing the Savin formula.[34−37] This states that the Raman intensity for mode i is proportional to $\Delta_i^2\omega_i^2$, where Δ_i and ω_i are the dimensionless displacement and the angular frequency for mode i, respectively. Turning now to the *adiabatic approach*, a geometry optimization (by quantum chemical methods) of both the ground and excited state is carried out, and the optimized geometries and Hessians of both states are used. Thus, in this approach, the potential surfaces are expanded around different points, namely, the optimized geometries of the respective electronic states. Warshel and Karplus[38] have provided expressions for obtaining the vibrational parameters from the data provided by the adiabatic approach. These parameters are then used in the same way as in the vertical Hessian approach to calculate optical absorption and Raman spectra.

The frequencies and dimensionless displacements obtained from the different approaches are listed in Table 4. As a first example, we consider the vibrational parameters of the radical cation of DMP-d_0 obtained via the vertical Hessian approach.

Table 4. Calculated Vibrational Frequencies (cm^{-1}) and Displacements for the Totally Symmetric Modes[a] of the Excited State of the Radical Cation of DMP-d_0, Compared with Its Ground State, Obtained with the Vertical Gradient, the Vertical Hessian, and the Adiabatic Approaches, Based on B3LYP/6-31G* Calculations[b]

vertical gradient[c] ω_e	vertical Hessian ω_e	adiabatic ω_e	vertical gradient $\lvert\Delta\rvert$	vertical Hessian $\lvert\Delta\rvert$	adiabatic $\lvert\Delta\rvert$
163	158	198	4.17	3.17	8.11
434	363	372	1.72	1.52	7.09
490	412	403	0.66	1.37	2.12
751	729	741	0.73	0.64	6.78
830	837	1010	2.17	1.43	10.23
986	1025	1060	1.27	0.82	8.71
1111	1099	1094	0.30	0.11	3.41
1158	1167	1146	0.46	0.43	6.88
1285	1335	1328	1.36	0.98	2.14
1362	1377	1412	0.07	0.10	4.99
1436	1418	1434	0.00	0.06	3.04
1469	1452	1460	0.12	0.08	2.63
1498	1477	1469	0.15	0.17	1.83

[a] C−H stretching modes are omitted. [b] All frequencies are scaled by a factor 0.974. [c] Identical to ground-state frequencies.

By using the calculated vibrational parameters (see Table 4) as input data for the time-domain formulation,[32] the optical absorption (Figure 1A) and resonance Raman (Figure 1B) spectra can be computed.

Parts A and B of Figure 1 provide a comparison between experimental and computed optical absorption and resonance Raman spectra of the radical cation of DMP-d_0. A good agreement between observed and calculated spectra is found. In particular, a good fit to the optical absorption spectrum confirms that the excited-state frequencies and the dimensionless displacements can be trusted. Parts C and D of Figure 1 show a comparison between the experimental and computed (using the vertical Hessian approach) resonance Raman spectra of the radical cations of DMP-d_4 and DMP-d_6. It is seen that the agreement for d_6 is very good, while that of d_4 is slightly worse in some parts of the resonance Raman spectrum.

A comparison of calculated resonance Raman spectra for the radical cation of DMP-d_0 using the different theoretical approaches is shown in Figure 7.

It is seen that while the vertical approaches reproduce the experimental observations reasonably well, the adiabatic approach is far off. Actually, many of the displacements obtained by the adiabatic approach are so large (see Table 4) that the harmonic approximation is considered not to be valid anymore. As can be seen in Figure 7, the unrealistically large displacements lead to very poor agreement between theory and experiment. Moreover, concomitantly with such large displacements, a substantial Duschinsky effect occurs, i.e., a rotation of vibrational modes between the ground and excited state. This large Duschinsky effect is the reason for the observation that in the adiabatic approach the modes with largest displacements not necessarily are the ones with largest RR intensities. The large difference between the dimensionless displacements of the vertical and adiabatic approaches clearly indicates that there is a high degree of anharmonicity of the excited-state potential energy surface in the region between the optimized geometry of the ground electronic state and that of the excited electronic state. Comparison of the geometry change on the excited-state surface predicted by the vertical Hessian approach with the actual result of geometry optimization (adiabatic approach) should also give an impression of the anharmonicity of the excited-state surface (see Figure 5). The excited-state geometry extrapolated using the vertical Hessian approach at the B3LYP

(32) Tannor, D. J.; Heller, E. J. *J. Chem. Phys.* **1982**, *77*, 202.
(33) Svendsen, C. Ph.D. Thesis, Odense University, 1997.
(34) Heller, E. J.; Sundberg, R. L.; Tannor, D. *J. Phys. Chem.* **1982**, *86*, 1822.
(35) Lee, S. Y.; Lee, S. C. *J. Chem. Phys.* **1992**, *96*, 5734.
(36) Wootton, J. L.; Zink, J. I. *J. Am. Chem. Soc.* **1997**, *119*, 1895.
(37) Myers, A. B. *Chem. Rev.* **1996**, *96*, 911.
(38) Warshel, A.; Karplus, M. *Chem. Phys. Lett.* **1972**, *17*, 7.

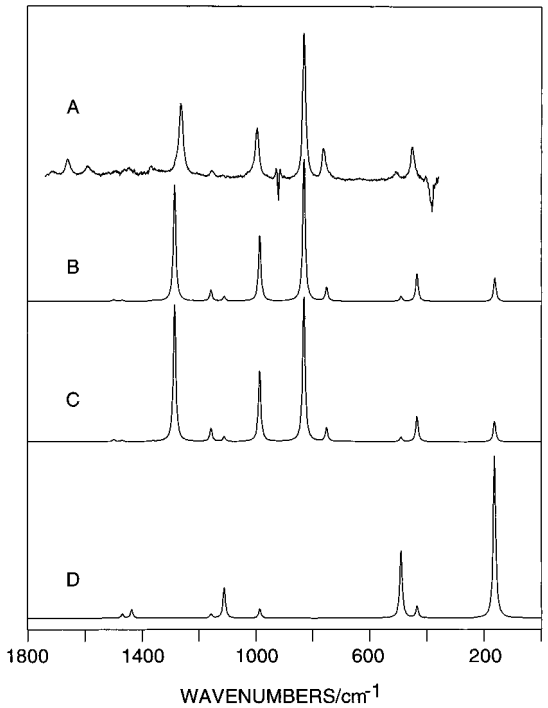

Figure 7. Comparison of different theoretical approaches: Observed and calculated resonance Raman spectra of the radical cation of DMP-d_0 using the vibrational parameters of Table 4. (A) Experimental spectrum (as Figure 1B), (B) calculated using the vertical Hessian approach, (C) calculated using the vertical gradient approach, and (D) calculated using the adiabatic approach.

level is 13.8 kcal/mol higher in energy than the fully optimized structure (adiabatic approach). It differs notably from the optimized structure in two respects: the C−C bond is much more shortened (1.495 Å vs 1.523 Å), and the change in pyramidalization of the nitrogens is much less developed (the amino group is essentially planar). Thus, it is understandable that the intensities of modes involving nitrogen inversion are overestimated in the adiabatic approach, while those involving C−C stretching are underestimated.

It is interesting to note that the Raman intensities predicted by the vertical gradient approach are rather close to the experimental ones. Table 4 contains the corresponding displacements. For most of the Raman active modes these displacements are larger than those predicted by the more sophisticated vertical Hessian approach. However, since only the relative Raman intensities are needed, it is only the relative size of the displacements that is important.

In the present case of DMP^+, the autocorrelators from which the spectra are computed[32] have a typical damping time of ca. 5 fs which is comparable to the vibrational period of the high-frequency C−H stretching modes. No phenomenological lifetime factor has been included in the autocorrelators, and hence the small damping time can only be attributed to the large number of vibrational degrees of freedom which are explicitly included in the autocorrelator. Because of the relatively short damping time, only the short time dynamics of the wave packet are important. This, in turn, means that only a small region of the excited potential surface around the equilibrium geometry of the ground electronic state contributes significantly to the optical absorption and resonance Raman scattering cross-sections. This is probably the reason the vertical approach works much better than the adiabatic approach for DMP^+. On the other hand, for small polyatomic molecules which often have long damping times, the adiabatic approach may yield the best result because the wave packet now samples information in a large region of the excited potential surface centered around the equilibrium geometry of the excited electronic state.

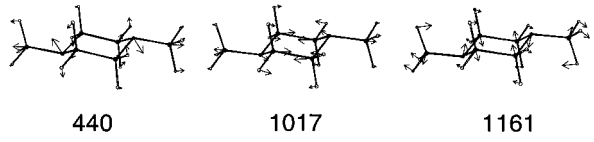

Figure 8. Normal modes of DMP (B3LYP/6-31G*) showing preresonance enhancement. Frequencies are experimental values (cm^{-1}).

Thus, we conclude that for the assignment of both Raman and optical absorption spectra the vertical Hessian approach is needed to obtain qualitatively correct results; if the interest is focused on the Raman spectrum only, then, at least in the present case of DMP^+, the vertical gradient approach yields reasonable results.

In our preliminary paper,[13] we noted that the intensities in the resonance Raman spectrum of DMP^+ were reproduced qualitatively by the HF/6-31G* computed *nonresonant* intensities, which may be attributed to the fact that the energy surface of the upper resonant state is the only low-lying excited-state surface that can contribute to the polarizability derivatives. Although the computed resonance Raman intensities are in much better agreement with experiment than the off-resonance intensities, the latter are computationally very easy to obtain, and may serve as a useful guideline. For example, the observation (section 6.1) that the Raman intensities computed for the twisted-boat forms do not agree with experiment can be taken as a further argument against them.

In this work we have used computation of the potential surfaces to interpret the resonance Raman spectra. The opposite procedure, in which excited-state displacements are derived from experimental resonance Raman intensities and normal-mode analyses, relies on the assumption that the excited-state surface is harmonic in the region between the Franck−Condon geometry and the excited-state energy minimum. This requirement is probably met in many cases,[36,37] but the present example of DMP^+ definitely summons for caution.

6.3. Raman Spectra of the Neutral DMP Molecule. Raman spectra of neutral DMP were obtained under preresonance conditions (266 nm) and off-resonance conditions (1064 nm, FT-Raman). They are shown in Figure 2. All bands can be readily assigned on the basis of HF/6-31G* calculations, from which Raman intensities are also available.

The calculations predict that in the spectral range 0−1700 cm^{-1} 13 a_g modes and 10 b_g modes are to be observed. A comparison of experimental and computed frequencies can be found in the Supporting Information. Here we merely wish to point out that three modes show a pronounced preresonance enhancement, viz., those giving rise to bands at 440, 1017, and 1161 cm^{-1}, while the strongest band in the off-resonance spectrum (777 cm^{-1}) is of only moderate intensity in the preresonance case. The three most active vibrational modes are graphically presented in Figure 8.

The present preresonance Raman data are not sufficient to derive the geometry changes upon excitation of DMP into its lowest excited singlet state. Calculations of this excited state have not been performed, but considering that it is of Rydberg nature,[39] one may expect it to structurally resemble the radical cation in many respects.[40] Thus, major geometry changes that are likely to occur upon excitation are in the pyramidalization

(39) Halpern, A. M.; Gartman, T. *J. Am. Chem. Soc.* **1974**, *96*, 1393.
(40) Zwier, J. M.; Wiering, P. G.; Brouwer, A. M.; Bebelaar, D.; Buma, W. J. *J. Am. Chem. Soc.* **1997**, *119*, 11523.

of the nitrogens, and in a lengthening of the C2−C3 bond. In Figure 8 it can be seen that such internal coordinates do indeed contribute significantly to the resonance enhanced modes. The structure of the excited state of DMP is currently being studied in more detail using high-resolution supersonic jet spectroscopy.

7. Conclusions

The establishment of the structure of molecular species that are too unstable to be handled under a variety of experimental conditions is a classical challenge in chemistry. Optical absorption and Raman scattering spectroscopy have the advantage that dynamical averaging of structures, e.g., two equivalent charge-localized structures in DMP^+, does not occur on the very short time scale of detection. What remains to be proven, though, is that the vibrational spectrum contains enough information to identify the correct structure and to reject other possibilities. In this process of identification one has to rely on methods to predict the vibrational spectra of all conceivable structures. At present, the only way to make such predictions is by ab initio quantum-chemical calculations. The computationally economic B3LYP/6-31G* methodology has proven to be successful for structures and vibrational spectra of neutral molecules, and in an increasing number of cases also for radical cations. Unfortunately, accurate experimental structural data of radical cations are scarce, so thorough testing of the performance of the calculation is not possible. On the other hand, many members of the scientific community have enough confidence in quantum-chemical methods to base predictions only on computational results. From this perspective, in the present case of DMP^+ the computed relative energies of the conceivable structures yield already persuasive evidence that the C_{2h} chair structure is the most stable, in the gas phase, but also in a polar solvent. A polar solvent tends to favor charge localization, but SCIPCM calculations indicate that in this case the solvation energy gain is insufficient.

Taking into account the excellent agreement of experimental and computed vibrational frequencies and also of the optical excitation energy for this structure, we conclude that we have established the molecular structure of the radical cation of *N*,*N*-dimethylpiperazine beyond reasonable doubt. Other conformations are predicted to have different spectra, and are at least 10 kcal/mol higher in energy.

A large geometry reorganization occurs in DMP after ionization, because the structure of the neutral molecule is unfavorable for through-bond interaction. In the relaxed radical cation, the lone pair orbitals of the amino groups interact strongly with each other and with the intervening σ-bond. The most characteristic structural features, i.e., the inverted pyramidalization of the amino groups and the lengthening of the C2−C3 (C5−C6) bond, are directly related to this TBI.

The resonance Raman intensities could be calculated very well using the vertical Hessian approach; i.e., wave packet propagation is performed on the excited-state potential energy surface expanded to second order around the ground-state geometry. When the model surface is generated by expansion around the optimized geometry of the excited state (adiabatic approach), incorrect results are obtained, due to the strong anharmonicity of the excited-state surface between the two geometries.

The preresonance Raman spectrum of neutral DMP reveals specific enhancements of a few a_g modes. Since the Rydberg-type excited state is likely to resemble the radical cation in many respects, this in principle should allow us to derive the corresponding geometry changes directly. The present experimental data are not sufficient to do this, but due to the emissive nature of the excited state of DMP, other spectroscopic methods can be used; in particular we will explore high-resolution gas-phase spectroscopy.

Acknowledgment. We thank Dr. Hans Hofstraat and Dr. Brenda Rossenaar (Akzo Nobel, Arnhem) for recording the FT-Raman spectrum of DMP. We have enjoyed several helpful discussions of the HF instability problem with Dr. Thomas Bally (Fribourg), Dr. Ria Broer (Groningen), and Dr. Ian Carmichael (Notre Dame). This research was sponsored by the Stichting Nationale Computer Faciliteiten (National Computing Facilities Foundation, NCF) for the use of supercomputer facilities, and supported (in part) by The Netherlands Foundation for Chemical Research (SON), with financial support from the Nederlandse Organisatie voor Wetenschappelijk Onderzoek (Netherlands Organization for Scientific Research, NWO). In addition, NWO provided a travel grant to A.M.B., which has been essential to initiate this work. Furthermore, this work was supported by a grant from the Danish National Science Research Council to the Center for Molecular Dynamics and Laser Chemistry. The authors thank K. B. Hansen, J. Fenger, E. Engholm Larsen, and J. F. Offersgård for valuable help with hardware and software, K. Bajdor for help with the measurements of the Raman spectra of the deuterated isotopomers, and T. Keszthelyi for help with the Raman intensity calculations.

Supporting Information Available: Optimized molecular geometries (HF/6-31G* and B3LYP/6-31G*) in Gaussian input format, and a table of experimental and computed frequencies of DMP (12 pages, print/PDF). See any current masthead page for ordering information and Web access instructions.

JA9735721